

Emittance Growth by Beam-Gas Scattering in Single Pass Accelerator

F. Le Pimpec^{*}, T. Schietinger

*Paul Scherrer Institute
5232 Villigen Switzerland*

Abstract

In order to ensure proper SASE lasing of a 4th Generation light source, one of the goal is to produce an electron beam of small emittance and to conserve it until its used in the machine undulator. One of the non recoverable emittance increase is the collision of the electron beam during its transport with the residual gas. Based on previous work by others, we have derived a useful expression of emittance increase for electrons of any energy and cross check its validity for energies above 100 MeV with an analytical formula.

Key words: Cross section, residual gas, emittance, Electron Source,
PACS: 29.27.-a, 34.80.Bm, 34.80.Dp

1 Introduction

In a single pass free electron laser accelerator (FEL) one of the key component is the electron source. The source should provide a sufficient amount of electrons and should have a low emittance which has to be preserved to provide the x-ray photons quality requested by the end users. A small emittance is paramount to reduce the electron energy necessary to lase. This of course implies a reduced cost for the machine.

Emittance growth happens through multiple channels [1]. We will only consider emittance growth produced by the interaction of the electron beam with the residual gas.

During their transport, the electrons will collide with the residual gas and the

^{*} Corresponding author

Email address: Frederic.Le.Pimpec@xfel.eu (F. Le Pimpec).

emittance will irreversibly increase. The residual gas pressure in a circular accelerator is usually sufficiently low that this process is negligible compared to other sources of emittance dilution. For SwissFEL, a fourth generation light source, the vacuum pressure might not be of a quality equivalent to that of a storage ring (3rd generation light source), as the beam will be discarded after use. The quality of the emittance is one of the most important parameters to obtain lasing [2].

The pumping scheme of the SwissFEL main Linac employs lump pumps at various location, mainly near the opening of the 2 m C-band and 4 m long S-band RF structures [2]. The dynamic pressure inside the machine might reach in a worst case scenario the low 10^{-6} Torr range. The question is to understand the quality level of the vacuum required in term of emittance dilution in order to not hamper proper lasing.

2 Emittance growth after collisions

Each electron after a collision with the residual gas will deviate from its original direction by an angle θ . The following is based on Raubenheimer's work [3,4].

The single-particle invariant before collision is :

$$A_x^2 = \gamma x^2 + 2\alpha x x' + \beta x'^2 \quad (1)$$

with $x(s)$ the position of the particle, $x' = \frac{dx}{ds}$, $\beta(s)$ the betatron function, $\alpha(s) = -\frac{1}{2} \frac{d\beta}{ds}$ and $\gamma(s) = \frac{1+\alpha(s)^2}{\beta(s)}$. A_x^2 is the emittance.

After a collision equation 1 becomes

$$\widetilde{A}_x^2 = \gamma x^2 + 2\alpha x(x' + \Delta x') + \beta(x' + \Delta x')^2 \quad (2)$$

From equation 1 and equation 2 and assuming $\langle x \rangle = 0$ and $\langle x' \rangle = 0$, we obtain :

$$\Delta A_x^2 = 2\alpha x \Delta x' + 2\beta x' \Delta x' + \beta \Delta x'^2 \quad (3)$$

The change in emittance ϵ after many collisions :

$$\Delta \epsilon - \langle \Delta A_x^2 \rangle - \beta \langle \Delta x'^2 \rangle \approx \frac{\beta}{2} \langle \theta_M^2 \rangle \quad (4)$$

$$\Delta\epsilon \approx \frac{\beta}{2} \langle \theta_M^2 \rangle \quad (5)$$

with $\langle \Delta A_x^2 \rangle$ averaged over the beam and θ_M^2 being the angle after multiple scattering [1]. The scattering between s and s+ds is then:

$$\langle \theta_M^2 \rangle = N\sigma ds \langle \theta^2 \rangle \quad (6)$$

with N the number of molecules on which the electron scatters, σ the total cross section of collision, which will include ionization and θ the single scattering angle. We obtain for the small angle approximation :

$$\langle \theta^2 \rangle = \frac{1}{\sigma} \int \theta^2 \frac{d\sigma}{d\Omega}(\theta) d\Omega = \frac{2\pi}{\sigma} \int \theta^3 \frac{d\sigma}{d\Omega}(\theta) d\theta \quad (7)$$

and for the emittance, when separating the total cross section and angular distribution we obtain the following equations.

$$d\epsilon = \pi N \beta(s) ds \int_0^{\theta_{max}} \frac{d\sigma}{d\Omega}(\theta) \theta^3 d\theta \quad (8)$$

$$d\epsilon = \pi N \beta(s) \sigma ds \int_0^{\theta_{max}} f_1(\theta) \theta^3 d\theta \quad (9)$$

where θ_{max} is the maximum scattering angle to be considered and f_1 is the single scattering angular distribution.

$$f_1(\theta) = \frac{1}{\sigma} \frac{d\sigma}{d\Omega}(\theta) \quad (10)$$

The emittance growth is then giving by equation 11

$$d\epsilon = \pi N \beta(s) \sigma(E[s]) ds \int_0^{\theta_{max}} f_1(\theta, E[s]) \theta^3 d\theta \quad (11)$$

Where

- * N: number of gas molecules per cm³.
- * $\beta(s)$: beta function between s1 and s2.
- * E(s): electron energy between s1 and s2.

- * $\sigma(s)$: electron gas cross section in the relevant energy range
- * $f_1(\theta, E)$: single scattering angular distribution in the relevant energy range.
- * Integration of $f_1 \times \theta^3$ up to θ_{max} , the largest relevant scattering angle (left to the user to define), as a function of E .

2.1 Gas molecule density

Using the ideal combined gas law, $N = P/(k_b T)$, at room temperature $T=300$ K, the number of gas molecules is :

$$N[m^{-3}] = 3.2 \cdot 10^{13} \times P[nTorr] \quad (12)$$

2.2 Electron cross Section

In a baked UHV system, the main molecules present are hydrogen and then carbon based molecules (methane, Carbon mono- and dioxide). The main culprit for emittance growth is attributed to the elastic scattering with the gas nuclei over the inelastic scattering (ionization and excitation) [4].

We will only consider the case of CO, and we will assume that this is the main gas present in the accelerator beam pipe. With this assumption, the emittance growth calculated is then overestimated, as the cross section of collision for CO, see Fig.1 is bigger than for hydrogen.

The total cross section measurement can be found up to 5 keV. Ionization cross section measurement range from below 1 keV and from 100 keV to 2.7 MeV. The elastic cross section and ionization cross section have been measured between 10 eV to 10 keV.

The theory Wentzel-Molière, and other models, expect constant cross section above 1 MeV [8,9].

The solution adopted for emittance growth estimate is to use the Browning [8] parametrization, between 0.1 keV to 30 keV. Below 0.1 keV, we use the Liu-Sun [7] parametrization (for σ_{tot}), scaled to match the Browning curve at 0.1 keV. Above 30 keV, we use the Wentzel-Moliere model, scaled to match the Browning curve at 30 keV.

For SwissFEL, we will consider the electrons at the exit of the RF photogun. Their energy is above 6 MeV.

According to Fig.1, the cross section is constant and is ~ 1 Mbarn (10^{-22} m²).

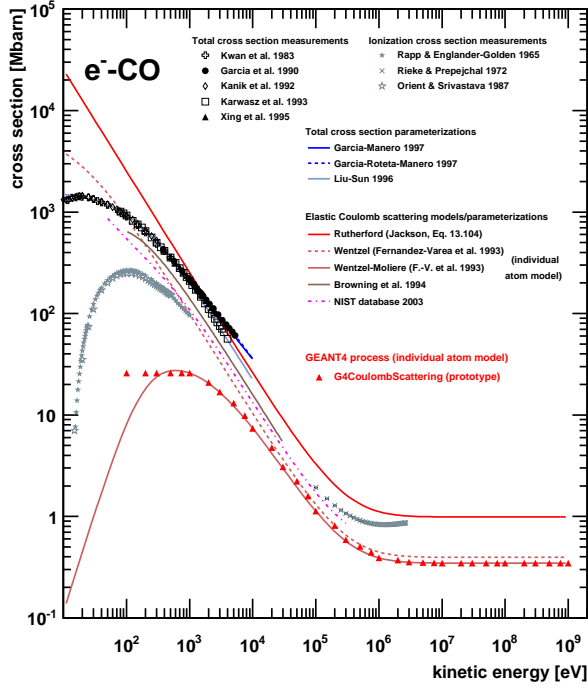


Figure 1. Electron - carbon monoxide (CO) total cross section [5,6,7,8,9].

2.3 Betatron function and energy

The betatron function $\beta(s)$ and the beam energy $E(s)$ are calculated along the designed machine using ASTRA and ELEGANT, see Fig.2 [10,11]. Given the optics we have used for some portion of the machine an average $\beta(s)$ and beam energy $E(s)$.

2.4 Single Scattering Angular Distribution

The function $f_1(\theta, E)$ is taken using the Wentzel-Molière model with the modified screening parameter (due to Molière), see Eq. (26) in Fernández-Varea et al [9] and reproduced here.

$$f_1(\theta) = \frac{1}{\pi} \frac{A(1+A)}{(2A+1-\cos(\theta))^2} \quad (13)$$

where

$$A = \left(\frac{\hbar}{2p} \right)^2 \frac{1.13 + 3.73(\alpha Z/\beta)^2}{(0.885 a_0 Z^{-1/3})^2} \quad (14)$$

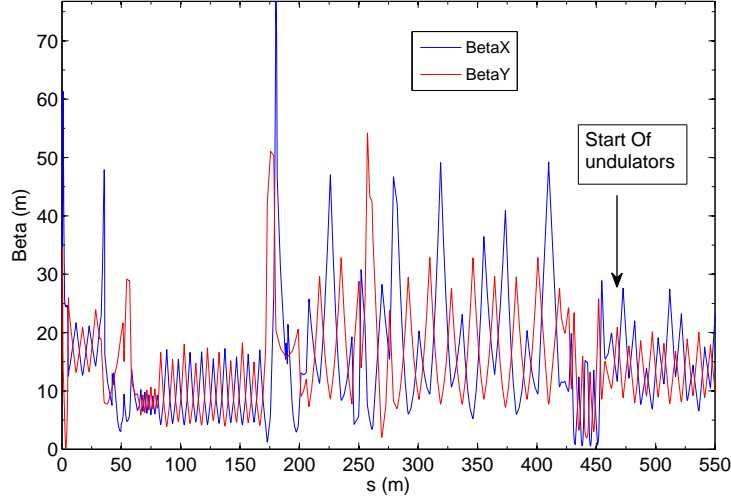


Figure 2. Beta X and Y function along the SwissFEL linac, Aramis beamline

A is the modified screening parameter [9], a_0 the classical electron radius, $\alpha=1/137$ the hyperfine constant for hydrogen, $\beta = v/c$ and Z the atomic number.

Wentzel-Molière model reproduces well the dependencies of the angular spread for an electron energy $E > 100$ keV when compared to measurement [12], as shown in Fig.3.

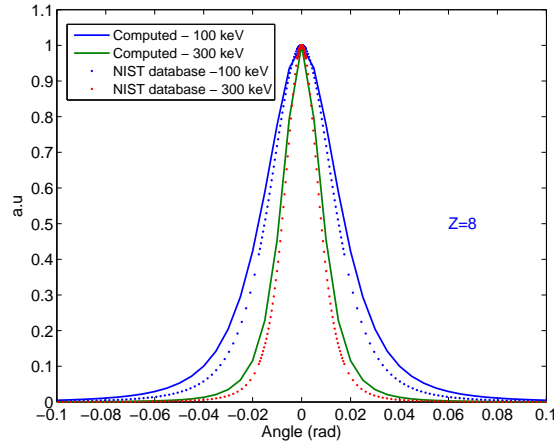


Figure 3. Comparison, for $Z=8$, between the measured and calculated distribution of $f_1(\theta)$. Measurement according to equation 10 and calculated using equation 14

For $E > 1$ MeV, the distribution of $f_1(\theta)$ are very similar for $Z=6, 7, 8$ and 14 as shown in Fig.4.

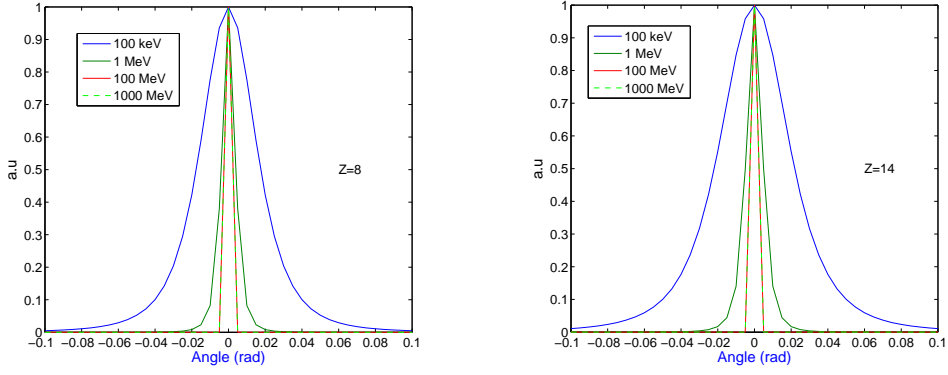


Figure 4. Single scattering angular distribution at different electron energies for $Z=8$ (left figure) and $Z=14$ (right figure)

2.5 Integration of $f_1 \cdot \theta^3$

From equation.11, we now need to integrate the last term as a function of the energy.

$$I(E) = \int_0^{\theta_{max}} f_1(\theta, E[s])\theta^3 d\theta \quad (15)$$

After the second S-band RF structure in SwissFEL, the beam energy E is above 100 MeV. From Fig.4, we can consider that a $\theta_{max}=0.1$ rad angle (5.7 deg) is a valid small angle approximation.

The numerical integration for an energy of 100 MeV and for CO, $Z=14$ (8 electron for the oxygen and 6 for carbon) is :

$$I(E = 100 \text{ MeV}) = 1.35 \cdot 10^{-8} \quad (16)$$

For energy above 100 MeV the value for single scattering angular distribution is smaller as the energy increases, see equation 14 and shown in Fig.4.

2.6 Normalized Emittance Increase

We will overestimate the emittance increase given by equation.11 by accepting that $I(E)$ is constant for energies above 100 MeV (equation 15) and is equal to $1.35 \cdot 10^{-8}$, equation 16.

Equation.11 now becomes :

$$d\epsilon = \pi \times N[m^{-3}] \times P(nTorr) \times \beta(s) \times \sigma(E[s]) \times I(E(s)) \quad (17)$$

The normalized emittance increase is then given by

$$d\epsilon_n = (\beta \times \gamma) \times d\epsilon \quad (18)$$

where β is the ratio of v to the speed of light c , and γ is the Lorentz factor ($\gamma = \frac{1}{\sqrt{1-\beta^2}}$).

For electrons having a total energy of 100 MeV ($E = \gamma m_0 c^2$), the lorentz factor $\gamma \sim 200$, β can be approximated by taking it equal to 1.

The numeric integration for CO, using a cross section $\sigma=0.5$ MBarn, Fig.1, a molecular density $N[m^{-3}]$ of $3.2 \cdot 10^{13}$, $I(E)=9.1 \cdot 10^{-9}$ equation.16, and an average beta function defined by the following :

$$\begin{aligned} \langle \beta \rangle [m] &= 12.8 \text{ for } 0 < s(m) < 170 \\ \langle \beta \rangle [m] &= 19.4 \text{ for } 170 < s(m) < 430 \end{aligned} \quad (19)$$

We obtain for the emittance increase the following :

$$\begin{aligned} d\epsilon_{0-170} [mm.mrad] &= 3 \cdot 10^{-7} P(nTorr) \\ d\epsilon_{170-430} [mm.mrad] &= 6.8 \cdot 10^{-7} P(nTorr) \end{aligned} \quad (20)$$

The normalized emittance is

$$\begin{aligned} d\epsilon_{n(0-170)} [mm.mrad] &= 200 \times d\epsilon_{0-170} = 6 \cdot 10^{-5} P(nTorr) \\ d\epsilon_{n(170-430)} [mm.mrad] &= 200 \times d\epsilon_{170-430} = 13.6 \cdot 10^{-5} P(nTorr) \end{aligned} \quad (21)$$

Using equation.21 for a uniform pressure in the machine of of $P \sim 1000$ nTorr, the normalized emittance increase is :

$$\begin{aligned} d\epsilon_{n(0-170)} [mm.mrad] &= 0.06 \\ d\epsilon_{n(170-430)} [mm.mrad] &= 0.136 \end{aligned} \quad (22)$$

The overall emittance increase can be sufficiently significant, given the emit-

tance requirement to obtain lasing. In the case of SwissFEL a normalized emittance better than 0.4 mm.mrad is required.

3 Emittance growth comparison

Using the following equation 23 for electrons from Reiser [1]

$$\frac{d\epsilon_n}{ds} = \frac{8\pi}{k} n_s \frac{Z_g^2 r_c^2}{\beta^3 \gamma} \ln(204 Z_g^{-1/3}) \quad (23)$$

with r_c the classical radius of the electron ($2.8 \cdot 10^{-15}$ m), n_s the atoms/m³, β and γ the relativistic factors, Z_g the atomic number of the atom or molecule and k a wave number. The normalized emittance ϵ is given in m.rad.

Before doing the numerical integration it is important to look at the validity of equation.23. For a total energy of 5 MeV, $\gamma \sim 10$. Below this value the emittance rises fast and asymptotically to infinity Fig.5. This equation models well the emittance increase for highly relativistic electrons. It breaks down at low energy.

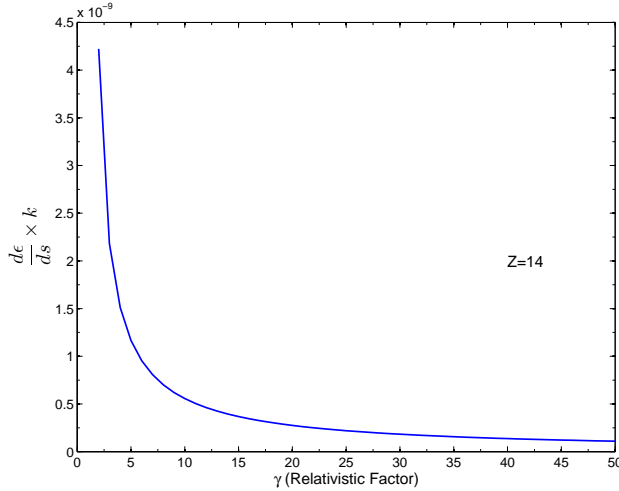


Figure 5. Variation of the normalized emittance, equation.23, in function of the particle energy (γ) for $Z=14$

The numerical integration for $Z_g=14$ (nitrogen molecule, or carbon monoxide); an electron beam energy of 100 MeV ($\beta \sim 1$ and $\gamma \sim 200$), with a linac length of 170 m, and a pressure of 1 nTorr, hence $n_s=3.2 \cdot 10^{13}$ at/m³. The average betatron value $\hat{\beta} = 1/k$ is 12.8 m, see equation 19. We obtain a normalized emittance (in mm.mrad) increase, normalized to $Z=14$:

$$d\epsilon_{n(0-170)} [mm.mrad] \sim 5.7 \times 10^{-5} \times (Z/14)^2 \times P[nTorr] \quad (24)$$

where Z is the atomic number of the element in the residual gas. For CO, the normalized emittance given by the Reiser [1] equation (equation.23) (0.0607 mm.mrad) is very close to the results obtained using equation.21.

4 Conclusion

We have derived a simple equation for an electron beam of any energy. The normalized emittance increased $d\epsilon_n$ can be obtained numerically at each position of the machine. The sum of the emittance increase will give the final increase of the emittance due to collision during the transport of the beam, for the partial pressure of one type of gas. The sum over all types of gases (characterized by their atomic number Z , and their partial pressure in the system) will give the overall emittance increase.

For energies above 100 MeV the analytical equation (Eq. 23) and our solution (Eq. 18) are in excellent agreement.

For low beam energy (below 1 MeV), however, care has to be taken in the approximation chosen. First the electron-residual gas cross section varies rapidly, see Fig.1. Second the small angle approximation should be revisited as the scattering angle increases for increasing atomic number (Z) and for low beam energy electron, Fig.4. These considerations limit also the application range of equation.18 due to the approximation taken for its determination. Such considerations would be applicable for DC gun for example [13].

5 Acknowledgments

We would like to thank A. Franchi (ESRF) for his very valuable input and critical look.

References

- [1] M. Reiser. *Theory and Design of Charged Particle Beams*. J. Wiley & Sons, 1994.
- [2] R. Ganter, editor. *SwissFEL Conceptual Design Report*. PSI-10-04. 2010.
- [3] T.O. Raubenheimer. The Generation and Acceleration of Low Emittance Flat Beams for Future Linear Colliders. Technical report, SLAC, 1991. SLAC Report 387.

- [4] T.O. Raubenheimer. Emittance growth due to beam-gas scattering. Technical report, KEK, 1991. KEK Report 92-7.
- [5] G. García, F. Manero. Correlation of the total cross section for electron scattering by molecules with 1022 electrons, and some molecular parameters at intermediate energies. *Chemical Physics Letters*, 280:419, 1997.
- [6] G. García, M. Rotetat, F. Manero. Electron scattering by N₂ and CO at intermediate energies: 1-10 keV. *Chemical Physics Letters*, 264:589, 1997.
- [7] Y. Liu, J. Sun. A semi-empirical formula for total cross sections of electron scattering from diatomic molecules. *Physics Letters A*, 222(4):233, 1996.
- [8] T.O. Browning et al. Empirical forms for the electron/atom elastic cross sections from 0.1 to 30 keV. *Journal of Applied Physics*, 76(4):2016, 1994.
- [9] J.M. Fernández-Varea et al. On the theory and simulation of multiple elastic scattering of electrons. *Nuclear Instruments and Methods in Physics Research B*, 73:447, 1993.
- [10] K. Flöttmann. A Space Charge Tracking Algorithm. <http://www.desy.de/~mpyflo/>.
- [11] M. Borland. accelerator simulation. http://www.aps.anl.gov/Accelerator_Systems_Division/Accelerator_Operations_Physics/oagSoftware.shtml.
- [12] NIST Electron Elastic-Scattering cross section Database - version 3.1. Technical report, NIST, 2003.
- [13] R. Ganter et al. Electron Beam Characterization of a combined diode rf electron gun. *Phys. Rev. Special Topics - Accelerators and Beams*, 13 (093502), 2010.

List of Figures

1	Electron - carbon monoxide (CO) total cross section [5,6,7,8,9].	5
2	Beta X and Y function along the SwissFEL linac, Aramis beamline	6
3	Comparison, for $Z=8$, between the measured and calculated distribution of $f_1(\theta)$. Measurement according to equation 10 and calculated using equation 14	6
4	Single scattering angular distribution at different electron energies for $Z=8$ (left figure) and $Z=14$ (right figure)	7
5	Variation of the normalized emittance, equation.23, in function of the particle energy (γ) for $Z=14$	9

